Trace gas and dynamic process monitoring by Raman spectroscopy in metal-coated hollow glass fibres

Timothy M. James, Simone Rupp and Helmut H. Telle

Quantitative capillary Raman spectroscopy measurements are described, in which improved speed and sensitivity for atmospheric trace gas analysis and real-time monitoring of catalytic hydrogen-exchange reactions were demonstrated.

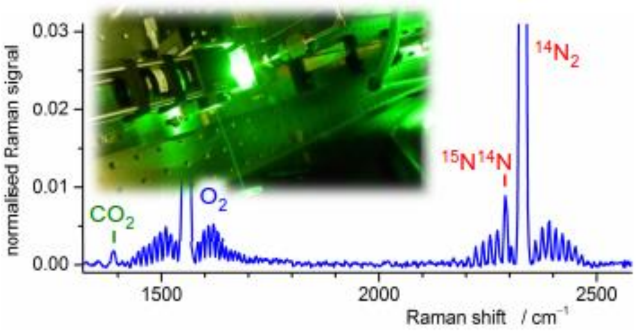

Analytical Methods

ARTICLE accepted for publication

Trace gas and dynamic process monitoring by Raman spectroscopy in metal-coated hollow glass fibres

Timothy M. James * [a], Simone Rupp [a] and Helmut H. Telle [b]

Results on using capillary Raman spectroscopy as an approach for improving the speed, sensitivity and limit of detection for quantitative analysis of gases are reported. Specifically, its potential for trace component identification and rapid process control has been explored. Using a metal-lined hollow glass capillary configuration, its Raman signal was found to be two orders of magnitude larger than that from a conventional 90° Raman implementation. However, the actual improvement in the signal-to-noise ratio and thus the limit of detection was markedly lower, due to an increase in the fluorescence background generated in optical components in the laser beam path and the capillary body itself. Using careful, systematic suppression strategies, the signal-to-noise ratio of our capillary setup increased by a further factor of 3-4, now yielding detection limits for trace gases well below the 100 ppm level. In a "dynamic" measurement series the time evolution of catalytic gas mixing of H_2 and D_2, to form HD, has been recorded, in which sub-mbar detection limits in sub-second recording times were achieved.

Introduction

Raman spectroscopy is a flexible technique that is used in a wide range of routine applications for the compositional analysis of solid and liquid samples. Raman analysis of gaseous samples has been less common, but with the advancement of laser and photon detector technology it has seen a significant increase in popularity over the last decade. To name but a few major, real-world applications to gas analysis, Raman spectroscopy is used for composition and temperature diagnostics in combustion systems (see *e.g.* Jourdanneau *et al* [1] and Kiefer *et al* [2]), in-line and real-time process control (see e.g. Marteau *et al* [3] and Csontos *et al* [4]), and measurements of atmospheric gas composition and aerosols based on Raman LIDAR systems (see *e.g.* Whiteman *et al* [5] and Müller *et al* [6]).

Development and applications in laboratory environments in general are based on gas cell arrangements, often in configurations in which the Raman light is observed at 90° with respect to the laser excitation. In favourable cases, detection limits of the order of just a few ppm have been reached for trace components in gaseous samples at atmospheric pressure.[7] Over the past ten years, we have set up and used a series of Raman systems for gas analysis applications at the Tritium Laboratory Karlsruhe (TLK), in particular to measure the composition of various mixtures of gaseous hydrogen isotopologues with high measurement precision, sensitivity and trueness.[8,9] These systems have a lower limit of detection (LOD), typically associated with a signal-to-noise ratio SNR = 3, of approximately 1 mbar/s (1 mbar in 1 s accumulation time). This is considered to be close to the ultimate reachable limit in 90°-configurations. However, for a number of envisaged applications of *e.g.* real-time information on trace molecules (sub-mbar) and/or faster feedback with the same pressure conditions, the Raman detection limit needs to be improved beyond that of current implementations. This may be achieved by (i) increasing the effective excitation laser power and/or by (ii) increasing the number of interacting molecules.

While increasing the primary laser power is within reach of modern laser systems, or local laser power can be increased within enhancement cavities,[10-12] one is often confronted with the limitation that the damage threshold to optical components, and/or their coatings, is reached. Increasing the number of contributing molecules can be achieved by either extending the lateral or longitudinal interaction volume; both approaches have their inherent advantages and caveats for collecting Raman light. An elegant and very promising approach to extend the interaction length, but at

[a] *Institute for Technical Physics (ITEP), Tritium Laboratory Karlsruhe (TLK), Karlsruhe Institute of Technology (KIT), P.O. Box 3640, 76021 Karlsruhe, Germany.*
E-mail: Timothy.James@kit.edu.
[b] *Instituto Pluridisciplinar, Universidad Complutense de Madrid, Paseo Juan XXIII-1, 28040 Madrid, Spain.*

† Electronic Supplementary Information (ESI) available: Additional details on some experimental aspects are provided, as well as a time-laps video of Raman spectral data of a circulating gas mixture. See DOI: 10.1039/xxxxxxxxxx

the same time maintaining decent light collection properties is to use metal-lined hollow glass fibres / capillaries as the Raman gas cell (also suitable for liquids, in principle).

Glass fibres with a hollow core were first identified in the 1960s as a useful tool to transmit and guide (high-power) laser and other light. They were internally coated with a thin metallic layer, so that the light propagates through this reflective-surface wave guide (see e.g. Eaglesfield [13]). Later, such fibres have been utilised not only to serve as a laser light guide, but to act as the actual Raman cell. The first mention of the principle goes as far back as 1996, outlined in an U.S patent.[14] In particular, the inventor highlights that the laser beam is not focussed into the capillary, but that it is collimated and thus prevented from interacting with the metallic coating, in order not to generate extra fluorescence and Raman features. For long glass fibres this would be next to impossible to realise: a "collimated'' beam of sub-mm diameter would normally exhibit non-negligible divergence. As a consequence, the laser beam would likely interact with the walls somewhere along the glass fibre. Thus, the glass fibre would have to be exceptionally straight and parallel to the beam to minimise interaction, and alignment would be extremely difficult.

Only a few years ago two US groups, at the University of South Carolina and at the National Energy Technology Laboratory, and one Japanese group at Tohoku University picked up on the principle, setting up, characterising and using silver-lined capillary Raman cells. The implementation by Pearman *et al* utilises fibre coupling of the laser excitation and Raman light collection.[15] In their tests with CO_2 and CH_4, they achieved 3σ-limits of detection of 0.3% and 0.02%, respectively, relative to their N_2 carrier gas.[16] Buric *et al* utilise direct-focussing in their implementation. They thoroughly characterised their setup,[17] and then primarily applied it as a sensor in gaseous fuel analysis at high pressure, with input feed pressures of up to 650 psig (44.8 bar).[18] In this application, the Raman measurement times were very short (0.1 s) to monitor the gas composition, therefore implying the potential for real-time combustion control. The Japanese group's main implementation aimed at compactness, coiling the capillary into a multiple loop of a few centimetres in radius. With their device they succeeded in human breath analysis, achieving detection limits of 0.2% variation in the O_2 content.[19]

Other fibre enhancement techniques have been investigated recently using hollow core photonic crystal fibres (PCF) as the Raman gas cell to extend the interaction length.[20,21] Hanf *et al* [20] utilise a purpose-manufactured fibre with a hollow-core diameter of about 7 μm, with the laser directly focussed into the core. They use the system as a sensor for early stage diagnostics of exhaled human breath [21], with a gas input system that allows cell pressures up to 20 bar, achieving excellent detection limits in the range 0.2-19 ppm for relatively short Raman measurement times. However, because of their extremely small hollow core, PCFs are not suitable for high-flow, inline monitoring applications, as is the case in our work: gas throughput would be insufficient and, in addition, severe differential pumping and gas separation effects would occur.

It is worth noting that techniques other than Raman spectroscopy are frequently used for the analysis of gaseous samples, and commercial instrumentation is now widely available. These alternatives include, for example, tuneable diode laser absorption spectroscopy (TDLAS) and mid-IR absorption spectroscopy utilising quantum-cascade laser (QCL) sources.[22,23] While these techniques exhibit very high sensitivity, with detection limits often down to the ppb-range, they have the drawback that very often a separate laser source is required, to resonantly probe each individual species in a gas mixture. Also, one might miss unexpected constituents in a gas mixture which lie outside the wavelength range of the particular excitation laser.

In this work, the concept of glass-capillary Raman spectroscopy has been investigated systematically, with the specific view to optimise its analytical performance, and to quantitatively compare setups utilising a Raman capillary with conventional 90° and forward / backward Raman spectroscopy implementations. In particular, we address issues related to fluorescence of optical components in the setup and the glass capillary itself, which – because of the increased shot noise – can severely dent the potential gain in signal because of a poorer signal-to-noise ratio. We include suggestions of how to minimise fluorescence in the optical system and at the same time maximising the collected Raman signal.

Raman trace gas measurements have been performed in (static) ambient air to show the high signal-to-noise ratio and low limit of detection (LOD) of the technique. The capillary Raman cell was also connected to a bespoke gas flow system, including a catalytic converter element, to monitor the mixing of hydrogen and deuterium and follow the catalytic conversion to HD in as close as possible to real-time.

Experimental setup

System configuration

A general optical setup for our capillary Raman cell is shown in Figure 1. For most of the measurements in this work, the laser is a 532 nm DPSS Nd:YVO_4 laser (Laser Quantum *Excel* or Coherent *Verdi V5*, providing 2 W or 5 W continuous wave output, respectively). The optional optical isolator can be used to prevent laser light reflecting back into the laser cavity; the λ/2 plate is used to adjust the polarisation of the beam for minimum reflection losses, off the 45° dichroic beam splitter. The laser beam is focussed via a "side-arm" configuration using a long focal length lens.

Various capillary lengths between 10 cm and 65 cm have been used, to allow for a range of systematic tests to be conducted. All capillaries were cut from lengths of hollow,

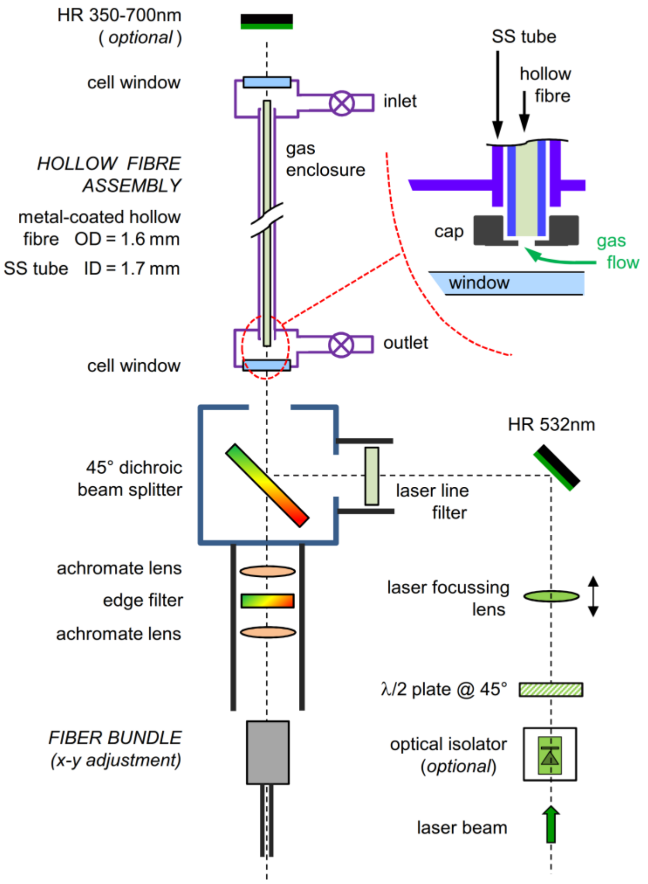

Fig. 1 Schematic sketch of the optical set-up for gas circulation capillary Raman measurements. HR = high-reflective mirror (optional). Insert: detail of the fibre – cap assembly.

silver-lined glass fibre, with an inner diameter of 1 mm and an outer diameter of 1.6 mm, optimised for wavelengths in the range 500-800 nm (Doko Engineering, VSS1000/1600). Note that the manufacturer also offers this silver lining with an additional polymer to improve the reflectivity and protect the silver coating from oxidation. In this work, no polymer coating was applied, due to the incompatibility of the coating with tritium. Oxidation of the silver is minimal because of the small diameter of the capillary, which leads to low air flow. Additional tests would need to be performed to assess the environmental resistance of the uncoated silver in more corrosive atmospheres. Both ends of the capillary are covered by a metal "cap" to prevent laser light from directly interacting with the capillary glass face. The central-hole diameter has been selected to minimise the fluorescence background, whilst capturing the Raman signal with minimal losses. Details on the cap optimisation process are outlined in Section S1.3 of the *Supplementary Information* document.

The laser beam enters and leaves the capillary through fused silica windows (of thickness 2-3 mm, AR-coating 400-800 nm), which seal the gas system. The (backward-scattered) Raman light from inside the capillary passes through the beam splitter, is collected by two achromatic lenses (with

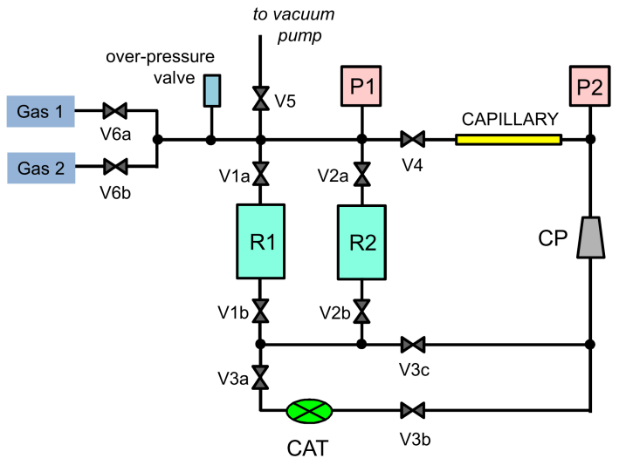

Fig. 2 Schematic sketch of the gas circulation system used with the capillary Raman cell. Vna,Vnb – bellow-sealed shut-off valves; R1,R2 – calibrated reservoir tanks; P1,P2 – pressure gauges; CAT – catalyst with Pt-coated alumina pellets; CP – circulation pump.

focal lengths of f = 75 mm and f = 60 mm, respectively) and imaged onto a fibre bundle (*CeramOptec*, 48 individual fibres of 100 μm core diameter, arranged in a custom "dot-to-slit" configuration, NA = 0.22). The collection-end of the bundle has a diameter of just less than 1 mm, similar to the capillary core diameter; the output end is arranged as a "slit" of the width of a single fibre and a height of about 6 mm. This matches the vertical sensor dimension of our CCD detectors (a variety of Princeton Instruments *Pixis* and Horiba *Synapse* devices were used).

The capillary is surrounded by a stainless steel (SS) tube with an outer diameter of 3 mm. On the one hand this serves as protection for the capillary fibre; on the other hand, each end of the SS-tube can easily be connectorised using appropriate fittings (in our case Swagelok tube fitting SS-3M0-1-2RS), to construct a vacuum-tight gas enclosure.

Gas-handling units can be connected to this capillary cell using inlet and outlet ports (see Figure 1 above). This could constitute a simple gas bottle – vacuum pump configuration, or a bespoke gas mixing system, as used for the real-time HD-mixing measurements discussed further below. The gas flow system utilised in this work is shown in Figure 2. It is designed in such a way that controlled amounts of gases can be filled into two custom-made reservoir vessels, R1 and R2, and then circulated through the capillary cell. In addition, one has the option to circulate the gas through a catalyst unit, or bypassing it, by opening and closing the valves labelled with the index "3", as required.

Note that all shut-off valves are bellow-sealed valves (Swagelok, SS-6BK-MM). Two pressure sensors P1 and P2 (SUNX, DP-100 series) allow for monitoring of the filling and circulation pressures. A low-pressure proportional relief valve (Swagelok, SS-RL3) is incorporated at the filling end of the circuit, set to release if the total pressure exceeds 1.5 bar. The circulation pump is a metal bellows pumping unit

(Metal Bellows Corp, MB-158E). The operation of this gas circulation loop is explained further below when discussing the dynamic mixing experiments in the results section.

Comparison strategy

To compare the improvements in signal-to-noise ratio when using the described capillary setup, as opposed to conventional 90° and forward / backward implementations, all operating parameters in the related measurements should be as close to equal as possible. Besides using the same spectrometer / detector system, in particular this holds for the settings of laser focussing and power.

In the related measurements, Raman spectra of air at atmospheric pressure were recorded, using the capillary cell with and without windows first, and then simply removing the cell for the 90° and forward / backward tasks. Note that the backward Raman measurements were made using the same input and collection configuration. For measuring the Raman spectra in the 90° configuration, our standard collection optics were installed,[24] such that the optics align with the focal point of the laser focussing lens. The "dot-to-slit" fibre bundle was disconnected from the spectrometer end and replaced with the "slit-to-slit" fibre bundle used in the 90° configuration.[25]

The spectroscopic data were acquired and analysed using our integrated acquisition and analysis routine *LARASoft*,[26] which combines the Raman acquisition routines with our post-acquisition cosmic-ray and background removal, as well as the peak fitting routines used in *SpecTools*.[27] Note that for the data discussed here, in selected spectra the background was not removed; this was specifically done to demonstrate changes in fluorescence contributions. In most cases, multiple back-to-back spectra were recorded and averaged for noise reduction. For real-time measurements (with individual acquisition times of the order 0.2-0.5 s), a "rolling average" procedure can be applied, the details of which are described further below.

Minimising fluorescence contributions

It is well known that, when the observation of Raman light is in the same or reverse (backwards) direction as the laser excitation, Raman and fluorescence light originating from optical components in the laser beam path always contribute to the observed scattering light intensity. Increased fluorescence will adversely influence the shot noise in the background spectrum, and the achievable signal-to-noise ratio will deteriorate; as a consequence, the LOD worsens. Thus it is paramount that any fluorescence is minimised as much as possible. If several optical components (such as lenses, windows and beam splitters) contribute to the fluorescence, its magnitude can easily be of the same order of magnitude as the collected Raman signal, or even larger. Further fluorescence may originate from the hollow glass fibre used to enhance the signal in capillary Raman spectroscopy setups. Primarily, it stems from the leakage of the (high power) laser light into the glass walls of the fibre, either through the inner metal coating or through the front face, and then propagating within the capillary glass, which implies that the majority of this fluorescence will emerge from the edges of the capillary.

The fluorescence introduced by optical components, which are exposed to laser radiation and are within the collection cone for Raman light, can be lowered by simply minimising the number of components. These can be reduced to only two (but no less) components, namely the dichroic beam splitter and the entrance window of the capillary cell (see Figure 1 above).

The two main variables of any optical component are the fabrication material and its thickness. The usual optical materials used in visible Raman spectroscopy are BK7, float glass, calcium fluoride or fused silica. Systematic test measurements have been performed that show that the fluorescence background level of fused silica – in line with expectations from literature data – is the lowest, followed by calcium fluoride, BK7, and finally float glass. The related, detailed results are collated in Section S1.2 of the *Supplementary Information*.

The fluorescence introduced by the capillary glass walls can be blocked from being collected by the spectrometer system, in principle. Okita *et al* [19] used a cap to cover the capillary wall face, while Mullen *et al* [28] coated the end facet of the capillaries with silver, to block the laser light from entering and the fluorescence light from exiting. In our setup we have used a cap with a central aperture of 0.8 mm diameter, which proved to be the optimal size down from the inner capillary diameter of 1 mm. For some additional details of the optimisation sequence see Section S1.3 in the *Supplementary Information*.

Note that for "open capillary" (*i.e.* no cell window) setups the capillary cap was replaced by a 0.8 mm pinhole, installed into an x-y adjustable mount. The centring location of the pinhole could then be optimised to ensure the fluorescence from the capillary was minimised, and hence the signal-to-noise ratio (SNR) was maximised. This centring adjustment proved to be advantageous for exact alignment, and it is envisaged to incorporate this concept into the closed cell as well, to allow for accurate centre-optimisation of the cap.

Finally, as mentioned in the introduction, the interaction of laser light with the capillary walls can be reduced by making the beam as collimated as feasible. The originally proposed full collimation [14] would be rather difficult to achieve. Therefore, we have opted for a long focal length lens, whose focal plane is located roughly at half the length of the capillary. Of course, the shorter the capillary the better the "collimation" associated with the focal depth parameter.

After all of the aforementioned minimising improvements have been implemented, the SNR had increased by a further factor of 3-4. For details related to all optimisation steps see Section S1 of the *Supplementary Information*. The important experimental parameters for the capillary Raman setup are

Table 1 Summary of the key capillary system parameters.

Variable	Description	Units	Value
Silver-lined hollow fibre (Doko, -*VSS*)			
L_C	Length	mm	650 (200, 100)
OD_C	Outer fibre diameter	mm	1.6
ID_C	Inner fibre diameter	mm	1.0
ID_{cap}	Cap pin hole	mm	0.8
	Internal coating		Ag (+ polycarbonate)
532nm DPSS laser (Laser Quantum *Excel* or Coherent *Verdi*)			
P	CW laser power	W	1–5
d_{laser}	Beam diameter (TEM_{00})	mm	1.8
f	Focal length of lens	mm	750

collated in Table 1experimental parameters for the capillary Raman setup are collated in Table 1.

Results and discussion

Detecting and quantifying trace gases in ambient air

To verify the sensitivity of the capillary system setup, the Raman system performance was tested with various gas mixtures; the simplest gas (mixture) to use is ambient air since its main constituent N_2 lends itself as a reference. In general, up to 100 acquisitions were made (for a 65cm-capillary cell, with 0.8 mm cap; laser power 1.5 W; Acton *SP500* or *SP2150* spectrometer).

The number of averages used for each measurement discussed in this work is explicitly stated. The effect of averaging on response speed and SNR is discussed below. In Figure 3 a typical background-corrected spectrum is shown, averaged over the full set of 100 acquisitions.

The spectrum clearly demonstrates the general sensitivity of the capillary setup. Not only are the weak O_1- and S_1-branches of N_2 and O_2 clearly visible and spectrally resolved, but one also can identify molecular specimen at trace level concentrations, namely CO_2, H_2O and the minor isotopologue of nitrogen, $^{14}N^{15}N$. Based on the aforementioned association of SNR = 3 with the limit of detection (LOD), and (i) assuming that at low particle densities the Raman signals scale linearly with concentration / pressure, and (ii) having cross-checked the variable atmospheric concentrations of CO_2 and H_2O, using the readings from an indoors CO_2 & humidity data logger (USB CO_2 data logger, *Perfect Prime*), one finds the following.

From the CO_2 peak at 1390 cm^{-1} (associated with the ν_1 symmetric stretch vibration), with a SNR ≈ 9, one deduces a LOD = 143 ppm, based on the laboratory air's CO_2 concentration of 430 (±5%) ppm; this means that one can trace about 0.1 mbar of CO_2 in a gas mixture of 1 bar.

From the amplitude of the H_2O peak at 3657 cm^{-1} (associated with the ν_1 symmetric stretch vibration), and based on a humidity / temperature measurements in the laboratory yielding the presence of water molecules at the level of about 1520 ppm (this is in the mid-range for an average humid day), one deduces a LOD = 400 ppm, or 0.4 mbar in a mixture of 1 bar. Note that the high-wavenumber range shown in the composite spectrum was recorded during a different measurement campaign, which utilised a lesser spectral resolution.

Finally, the measurement had sufficient spectral resolution and was sensitive enough to reveal the minor isotopologue of

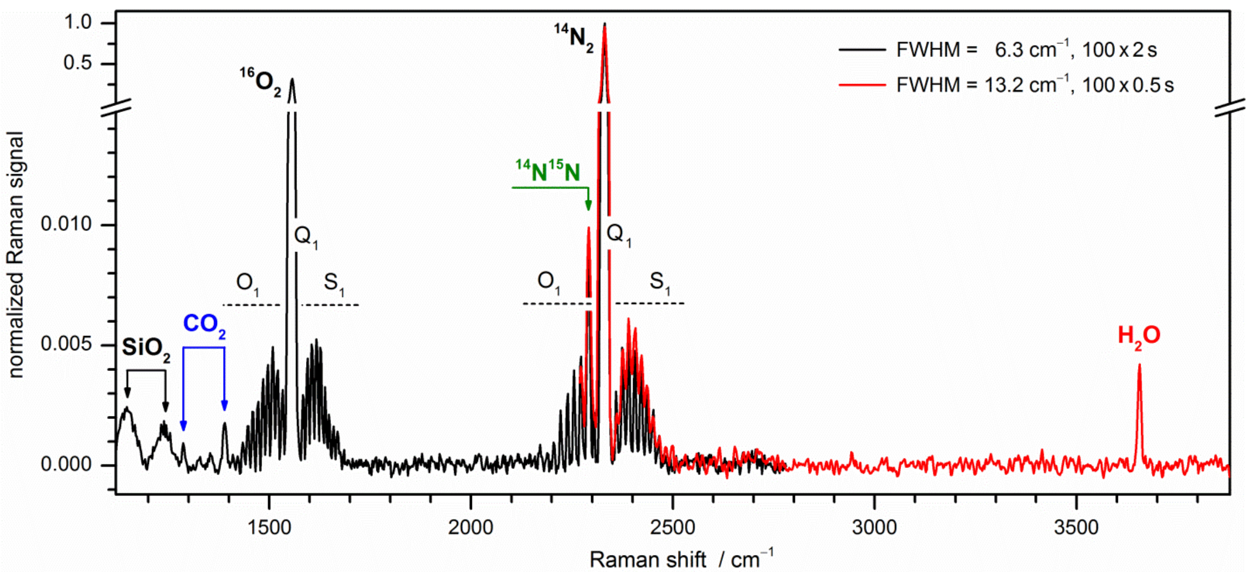

Fig. 3 Capillary Raman spectrum of air at atmospheric pressure, averaged over 100 acquisitions of 2 s (0.5 s) each. For nitrogen and oxygen, their Q_1-, O_1- and S_1-branches are highlighted; the Q_1-branch of the minor isotope $^{14}N^{15}N$ coincides with the O_1(J=5,6)-lines of $^{14}N_2$. For all other constituents, the peaks are only labelled for the species: SiO_2 (its fundamental stretching modes); CO_2 (Fermi-diad, ν_1 symmetric stretch and $2\nu_2$ bending overtone); H_2O (ν_1 symmetric stretch). The large-shift part (red trace) was recorded at lower spectral resolution.

nitrogen, $^{14}N^{15}N$. Note that simply integrating the respective Q_1-branches areas from the spectrum in Figure 4 would not yield the expected relative abundance of the $^{14}N^{15}N$ isotopologue. One first needs to deconvolute its Q_1-branch feature from the overlapping $O_1(J)$-branch lines of $^{14}N_2$. Doing this yields a relative abundance of 0.0074 ± 0.0003, in good agreement with the natural abundance in air.

For further details on the quantification of all components in the sampled air spectra see Section S2.1 in the *Supplementary Information*.

In addition to testing the performance of the capillary Raman system for LODs in gas mixtures, exemplified for air, we also performed a direct comparison between capillary Raman, and standard 90° (sideways) and 180º (backward) implementations without any cell, using the same laser settings, and the same spectrometer/detector combination. These comparison data were recorded for acquisition times in the range 0.1-2.0 s for all three experimental setups, averaging only five measurements for each case. The Raman signal amplitude was extracted as the height of the Q_1-branch of nitrogen and the noise as the standard deviation of a flat region of the background. The detection limit improvement is derived by calculating the SNR for any particular setting. The results from all data sets are summarised in Section S2 of the *Supplementary Information*. Here we discuss only one example, namely for incident laser power of 1 W at 532 nm, and an acquisition time of 2 s; the related, normalised N_2-spectra are shown in Figure 4. Note that the data shown in this figure were obtained before all of the discussed fluorescence background reduction measures were implemented, and before using a higher-sensitivity spectrometer/detector combination. A capillary cap with a central aperture of 1 mm diameter was used rather than the optimal 0.8 mm. The input laser light focal length was f = 150 mm rather than the optimal f = 750 mm, and the lens was exposed to laser radiation and installed in the Raman light collection cone. The comparison measurements were performed for this non-optimal configuration to provide a reference for the detection limit improvement and to enable further enhancement to be more easily quantified.

From the spectral data in the figure one finds a signal amplitude gain of ~16 and ~170, respectively, when changing from the standard 90° setup to the 180º backward or the capillary configurations. However, both backward configurations exhibit substantially increased noise when compared to the virtually fluorescence-free 90° setup. This is evidenced when comparing the base line in the capillary measurement with that of the (enlarged) baseline for the 90°-configuration: the shot noise is about a factor ×20 larger.

Thus, when taking the shot noise level into account, one finds that the detection limit improvement is far less than the signal amplitude gain for constituent molecules. Instead of the aforementioned signal amplitude gains of ~16 and ~170, one obtains a SNR improvement of only ~4 and ~9, respectively, for this particular measurement. This result clearly emphasises the need to understand and minimise fluorescence background contributions.

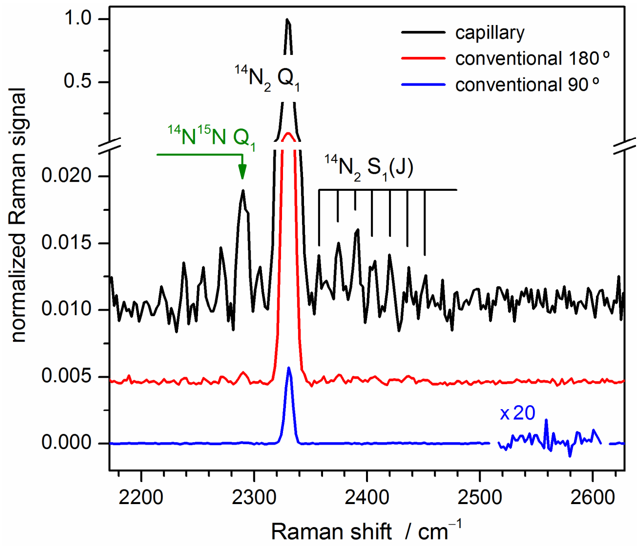

Fig. 4 Direct comparison of background-corrected Raman spectra of nitrogen in ambient air for our capillary – top (black) trace; conventional 180° – middle (red) trace; and conventional 90° – bottom (blue) trace – setups. For all configurations five acquisitions of 2 s each were averaged, and the spectra are normalised to the maximum of the capillary data; traces are offset for clarity.

In our final capillary system implementation (after all of the fluorescence background measures have been applied) the actual detection limit improvement was substantially higher (×90-100 as opposed to about ×24), albeit still being lower than the signal amplitude enhancement of ×170 one would have hoped for. The observed increase in the signal and SNR when using a capillary as the Raman cell is due to the extended optical path length (65 cm with capillary rather than ~1 cm without it) on the one hand, combined with greatly improved collection efficiency over the entire path length on the other hand.

Dynamic monitoring of gas mixtures, including catalytic conversion

In addition to the static high-sensitivity measurements we wanted to demonstrate that, when using the capillary Raman setup, the speed of detection would be sufficient to make the approach suitable for rapid process control. For this the capillary was connected to a (catalytic) gas mixing and circulation unit. Note that in our work related to the KATRIN (Karlsruhe TRItium Neutrino mass) experiment,[8] we built a gas mixing unit in which precise amounts of H_2 / D_2 fillings could be circulated. When passing the mixture through a catalyst vessel, filled with platinum-coated alumina pellets, the isotopologue HD is formed (for more details on this catalytic HYDE-loop see Schlösser *et al*[29]).

The dynamic monitoring measurements discussed here were performed with a 60 cm capillary, in single-pass con-

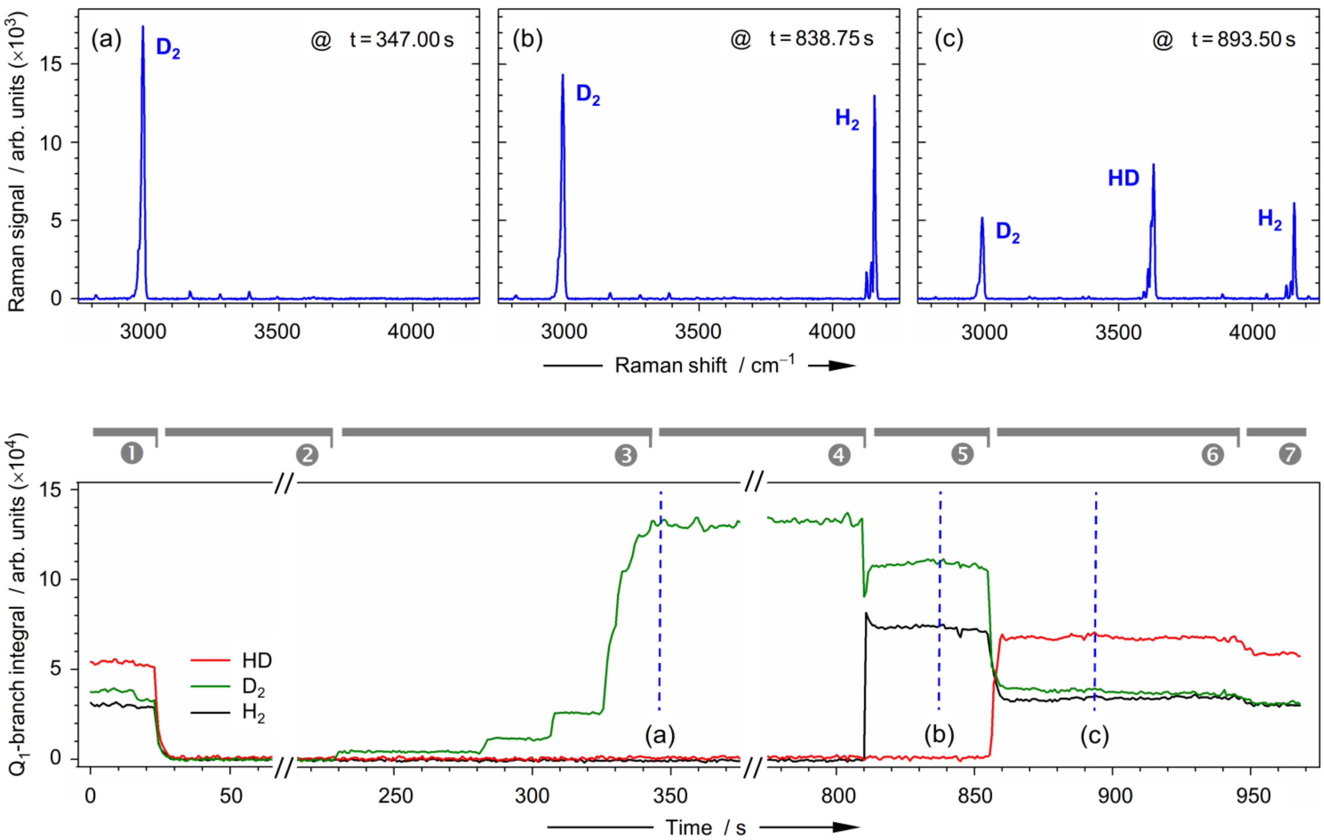

Fig. 5 Monitoring of the filling and (catalytic) mixing process for circulating hydrogen isotopologue mixtures, linked to the integral intensities of the Q-branches, as a function of time. Time steps are in multiples of 0.75 s (sum of 0.5 s acquisition time and ~0.25 s processing time). The numbers ❶ to ❼ correspond to the steps as described in the text. Snapshots of Raman spectra at selected times in the overall record are shown in top panels (a) to (c).

figuration (*i.e.* without the back-reflecting mirror shown in Figure 1). The mixing unit used here for demonstration purposes (see Figure 2 above) is based on the same principle as the HYDE loop but its volumes were not fully calibrated. The Raman spectra were acquired (and processed) continuously during the filling procedure and during circulation, using our integrated acquisition and analysis software *LARASoft*.[26] The accumulation time for each individual Raman spectrum was 0.5 s, with about a further 0.25 s in processing time.

An example for a full sequence of preparing, filling, and circulating gas mixtures including catalytic conversion is shown in Figure 5. The time record traces the relative abundance of the three isotopologues; at a few selected times Raman spectra, from which the abundance is calculated, are shown in panels (a) to (c). The numbered sequence shown in the figure (phases 1 to 7) is briefly described below, with a detailed description in Section S2.3 of the *Supplementary Information*.

Initially, during phase 1, spectral contributions for a previous gas mixture were recorded. That mixture was removed when completely evacuating the loop (phase 2 in the sequence), and consequently the Raman signals approached zero. During phase 3, D_2 was stepwise admitted to the system, up to a final D_2 pressure of 1000 mbar (for the demonstration of pressure changes here reference vessel R1 was open to the capillary so that measurement data could be recorded; normally, only the vessel would be filled to maintain calibration). During phase 4 for several minutes the D_2 signal was recorded to ascertain any measurement fluctuations; during this period the isolated second reference vessel R2 was filled with H_2, also to a pressure of 1000 mbar. At the beginning of phase 5, the H_2 was allowed to join into the system, and the circulation pump was switched on. Synchronous to the pump switch-on one could observe an initial pressure surge – which was reflected in the Raman signal as well. This is not surprising since the capillary with 1 mm inner diameter constitutes a noticeable pump cross section restriction with respect to the tubing of the loop, with 4 mm inner diameter. After a short time, the pressure reached equilibrium. In the following phase 6, the catalyst vessel was switched into the loop; the isotopologue HD started to appear rapidly while D_2 and H_2 diminished as a consequence of the catalytic conversion. The relative abundance of the three isotopologues equilibrated, after about 6.5-7.0 s. Taking into account the total system volume of ~700 cm^3 and the pumping speed of the MB-158E circulation pump of ~365 cm^3/s, nearly full catalytic conversion of the gas mixture was reached after just three circulations of the gas volume through the catalytic converter. Finally, the circulation pump was switched off again, and the static mixture was left for further monitoring (phase 7).

Overall, the data shown in Figure 5 demonstrate that our capillary Raman system is capable to follow rapid changes of gas composition and pressure, on the time scale of less than 1 s or even lower; thus it is quite suitable for process control, in principle. It is also sensitive enough to reveal even small traces of molecules (not visible on the scale shown in the figure). The spectral intensity data shown here can be converted into partial pressure information. Based on the reservoir / system filling volumes and pressures for H_2 and D_2 (for details see Section S2.3 of the *Supplement Information*) we derived a detection limit (SNR = 3) for the hydrogen isotopologues of 2.3 ± 0.4 mbar for an acquisition time of just $2{\times}0.5$ s.

At this point we would like to stress again that the achieved detection limits were not only influenced by the fluorescence reduction measures discussed above, but also by the choice of spectrometer / detector combination. In relation to implementing either or both of these two aspects the product LOD·t will become lower with each measure of improvement. As a consequence one may aim either (i) at bettering the LOD while keeping the acquisition time the same, or (ii) at shortening the measurement period to reach a specific LOD. For example, the above-stated value of 2.3 mbar in 1 s improved to <0.6 mbar in 1 s when changing from the *SP500* spectrometer / *Synapse* detector to the *SP2150* spectrometer / *Pixis 400* detector combination. Some extended discussion related to this issue is provided in Section S1.5 of the *Supplementary Information.*

Finally, it is also interesting to note that the data reveal differential pumping of gases with a different mass through a pumping restriction, as evidenced by the small, initial "kink" in the composition data for D_2 and H_2 at the point when H_2 is admitted to the system and the circulation pump is switched on (transition from phase 4 to phase 5). To better visualise the whole process, a time-lapse "movie" of the spectra of the discussed data set is provided as part of the *Supplementary Information*.

"Rolling average" procedure

As a final aspect of this investigation we present an approach how to improve the signal-to-noise ratio of the measured spectra, whilst not sacrificing much of the short-response time. In general, increasing the measurement time, i.e. averaging over a series of acquisitions, improves on the SNR; but as a consequence, speed is lost.

To overcome this detrimental effect we applied a "rolling average" to the data. This procedure consists of averaging a set number of consecutive spectra (S_1 to S_n). Then the next recorded spectrum replaces the first spectrum in the set, and this new set of spectra (S_2 to S_{n+1}) is averaged, and so on. This procedure has been applied to the data shown from Figure 5 above, with n = 2, 5 and 10. The effect of this procedure is shown in Figure 6 for the HD data sub-set, in the transitional region when catalysis of the H_2/D_2 mixture commences.

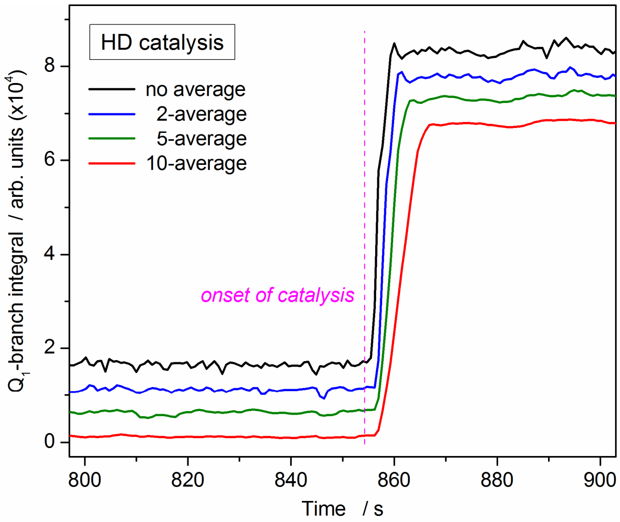

Fig. 6 Excerpt from the HD-concentration data from Fig. 6, but treated by rolling-average procedure, for averaging 2, 5 and 10 sets of data. The traces are offset to each other for clarity.

The figure shows that applying a rolling average to the data does smooth the signal respective to its shot noise, and small concentration variations begin to become recognisable, on the original sub-second time scale. On the down side, of course, one experiences a (minor) deterioration in the response speed to large, sudden changes in signal amplitude, as evidenced in the transition region from H_2/D_2 mixtures to a fully equilibrated isotopologue H_2/HD/D_2 mixture after passage through the catalyst. However, the transition slope has only slightly deteriorated from ~6.5 s to ~11 s in the case of 10 averages, albeit with a short delay, while at the same time the apparent noise fluctuation has reduced significantly more (by a factor of $\sqrt{10}$).

Conclusions

This work has been directed toward improving on the speed, sensitivity and limit of detection for quantitative Raman spectroscopy of gaseous samples, specifically aiming at trace components and the potential suitability for process control. The Raman signal enhancement afforded by our capillary cell implementation is in line with, if not superior to the results of other groups who have utilised metal-lined hollow glass capillaries in the past.

We have systematically investigated factors which adversely impact on the (quantitative) detection capabilities, in contrast to only aiming for the highest gain in Raman signal amplitude. It was found that primarily fluorescence generated (i) in optical components within the laser beam path, and (ii) in the capillary body itself did significantly affect the signal-to-noise ratio (SNR). We demonstrated that the SNR could be at least bettered by a factor of three when including measures such as (i) to reduce the number of optical elements in the laser beam path to the lowest possible minimum; (ii) to carefully select the material and the thickness of these components; and (iii) to suppress the capillary fluorescence by optimally machined metal caps.

The capillary results were compared to backward / forward measurements without a capillary, and to recordings under standard 90º-observation configuration. All data were collected using the same Raman excitation and detection equipment, and using directly comparable measurement conditions (1000 mbar total pressure; laser power of 1-2 W; and signal accumulation 10-100 s). We demonstrated that even without major optimisation in setup geometry and suppression of fluorescence, our capillary Raman setup proved superior to other configurations. Trace molecule components could be monitored to the order of 0.1 mbar, within a 1000 mbar gas mixture, using our pre-optimisation setup (most of the data discussed in the "Results" section). After implementation of the aforementioned improvements to significantly reduce the fluorescence background, the SNR could be increased by a factor of 3-4, depending on the wavelength region. Now for some trace molecules detection limits of the order of 0.03 mbar in 1000 mbar were obtained, *i.e.* well below the 100 ppm mark. And finally, in our dynamic measurement series of catalytic gas mixing, sub-mbar detection limits for sub-second recording times were achieved. Clearly, this supports our suggestion that capillary Raman spectroscopy has the potential to become useful in rapid, sensitive gas process control.

It has become quite clear that the adverse effect of component fluorescence is the major contributor which limits the achievable detection limit in glass capillary Raman setups. Beyond the measures for reduction employed in this study, full elimination of all fluorescence would be the most desirable. For example, commercial instruments targeting Raman spectroscopy of biological samples – in which fluorescence often dominates – use excitation lasers at longer wavelengths (usually 780 nm or 830 nm, instead of 532 nm). At those longer wavelengths bulk fluorescence in glasses normally decreases; however, one is faced with a severe decrease in Raman signal amplitude which follows the approximate ν^4-law. We are currently exploring different approaches of how to further lower the fluorescence background well below the currently achievable levels. First results are very promising, and thus the possibility for sensitive sub-second process control based on Raman spectroscopy seems to be within reach.

Finally, we like to note as well that at present cavity enhanced Raman spectroscopy for gases gains in popularity (see e.g. Salter *et al* [10], Keiner *et al* [11] or Frosch *et al* [12]). However, while achieving a high SNR and low detection limits, to our knowledge such systems are yet unproven in long-term monitoring and process-control applications in "harsh" environments, rather than within a well-controlled laboratory, or for use with corrosive gases (like e.g. tritium-containing mixtures investigated at KIT [26]).

Acknowledgements

Part of this work was supported by the Karlsruhe School of Elementary Particle and Astroparticle Physics: Science and Technology (KSETA) via a doctoral training grant for SR. Note that until the end of 2013 TMJ and HHT were affiliated with the Department of Physics, Swansea University, UK.

References

1 E. Jourdanneau, F. Chaussard, R. Saint-Loup, T. Gabard and H. Berger, *J. Mol. Spectrosc.*, 2005, **233**, 219-230.
2 J. Kiefer, T. Seeger, S. Steuer, S. Schorsch, M.C. Weikl and A. Leipertz, *Meas. Sci. Technol.*, 2008, **19**, 085408.
3 P. Marteau, N. Zanier-Szydlowski, A. Aoufi, G. Hotier and F. Cansell, *Vib. Spectrosc.*, 1995, **9**, 101-109.
4 I. Csontos, H. Pataki, A. Farkas, H. Bata, B. Vajna, Z.K. Nagy, G. Keglevich and G.J. Marosi, *Org. Process Res. Dev.*, 2014, doi: 10.1021/op500015d.
5 D.N. Whiteman, M. Cadirola, D. Venable, M. Calhoun, L. Miloshevich, K. Vermeesch, L. Twigg, A. Dirisu, D. Hurst, E. Hall, A. Jordan and H. Vömel, *Atmos. Meas. Tech. Discuss.*, 2011, **4**, 7337-7403.
6 D. Müller, I. Veselovskii, A. Kolgotin, M. Tesche, A. Ansmann and O. Dubovik, *Appl. Opt.*, 2013, **52**, 3178-3202.
7 P.G. Papageorgas, D. Maroulis, H. Winter, S.A. Karkanis, H. Albrecht and N.G. Theofanous, *IEEE Trans. Instrum. Meas.*, 2004, **53**, 58-66.
8 S. Fischer, M. Sturm, M. Schlösser, B. Bornschein, G. Drexlin, F. Priester, R.J. Lewis and H.H. Telle, *Fusion Sci. Technol.*, 2011, **60**, 925-930.
9 M. Schlösser, S. Rupp, H. Seitz, S. Fischer, B. Bornschein, T.M. James and H.H. Telle, *J. Mol. Struct.*, 2013, **1044**, 61-66.
10 R. Salter, J. Chu and M. Hippler, Analyst, 2012, 137, 4669-4676.
11 R. Keiner, T. Frosch, T. Massad, S. Trumbore and J. Popp, *Analyst*, 2014, **139**, 3879-3884.
12 T. Frosch, R. Keiner, B. Michalzik, B. Fischer and J. Popp, *Anal. Chem*, 2013, **85**, 1295-1299.
13 C.C. Eaglesfield, *Proc. IEE – Part B*, 1962, **109**, 26-32.
14 J. R. Mitchell, Diode laser pumped Raman gas analysis system with reflective hollow tube gas cell, 1996, U.S. Patent 5,521,703.
15 W.F. Pearman, J.C. Carter, S.M. Angel and J.W.J. Chan, *Appl. Spectrosc*. 2008, **62**, 285-289.
16 W.F. Pearman, J.C. Carter, S.M. Angel and J.W.J. Chan, *Appl. Opt.*, 2008, **47**, 4627-4632.
17 M.P. Buric, K.P. Chen, J. Falk and S.D. Woodruff, *J. Opt. Soc. Am. B*, 2010, **27**, 2612-2619.
18 M.P. Buric, B.T. Chorpening, J.C. Mullen, S.D. Wood¬ruff and J.A. Ranalli, IEEE Future of Instrumentation International Workshop (FIIW), 2012, doi: 10.1109/FIIW.2012.6378319.
19 Y. Okita, T. Katagiri and Y. Matsuura, *Proc. SPIE*, 2010, **7559**, 755908, doi:10.1117/12.841414.

20 S. Hanf, R. Keiner, D, Yan, J. Popp and T. Frosch, *Anal. Chem*., 2014, **86**, 5278 – 5285.

21 S. Hanf, T. Bögözi, R. Keiner, T. Frosch and J. Popp, *Anal. Chem*., 2015, Article ASAP doi: 10.1021/ac503450y.

22 J. Chen, A. Hangauer, R. Strzoda, M. Fleischer and M.C. Amann, *Opt. Lett*., 2010, **35**, 3577-3579.

23 C. Charlton, B. Temelkuran, G. Dellemann and B. Mizaikoff, *Appl. Phys. Lett*. 2005, **86**, 194102.

24 T.M. James, M. Schlösser, S. Fischer, M. Sturm, B. Bornschein, R.J. Lewis and H.H. Telle, *J. Raman Spectrosc*., 2013, **44**, 857-865.

25 M. Sturm, M. Schlösser, R.J. Lewis, B. Bornschein, G. Drexlin and H.H. Telle, *Laser Phys*., 2010, **20**, 493-507.

26 M. Schlösser, B. Bornschein, S. Fischer, T.M. James, F. Kassel, S. Rupp, M. Sturm and H.H. Telle, "Raman spectroscopy at the Tritium Laboratory Karlsruhe", *Fusion Sci. Technol*., 2015, **67**, in press.

27 T.M. James, M. Schlösser, R.J. Lewis, S. Fischer, B. Bornschein and H.H. Telle, *Appl. Spectrosc*., 2013, **67**, 949-959.

28 J.C. Mullen, M.P. Buric, B.T. Chorpening and S.D. Woodruff, *Opt. Eng*., 2013, **52**, 117103.

29 M. Schlösser, H. Seitz, S. Rupp, P. Herwig, C.G. Alecu, M. Sturm and B. Bornschein, *Anal. Chem*., 2013, **85**, 2739-2745.